MINIMUM VOLUME SIMPLICIAL ENCLOSURE FOR SPECTRAL UNMIXING OF REMOTELY SENSED HYPERSPECTRAL DATA

Eligius M.T. Hendrix, Inmaculada García

Department of Computer Architecture
University of Málaga
E-29071 Málaga, Spain

Javier Plaza, Antonio Plaza

Department of Computer Science
University of Extremadura
E-10071 Cáceres, Spain

ABSTRACT

Spectral unmixing is an important task for remotely sensed hyperspectral data exploitation. Linear spectral unmixing relies on two main steps: 1) identification of pure spectral constituents (endmembers), and 2) endmember abundance estimation in mixed pixels. One of the main problems concerning the identification of spectral endmembers is the lack of pure spectral signatures in real hyperspectral data due to spatial resolution and mixture phenomena happening at different scales. In this paper, we present a new method for endmember estimation which does not assume the presence of pure pixels in the input data. The method minimizes the volume of an enclosing simplex in the reduced space while estimating the fractional abundance of vertices in simultaneous fashion, as opposed to other volume-based approaches such as N-FINDR which inflate the simplex of maximum volume that can be formed using available image pixels. Our experimental results and comparisons to other endmember extraction algorithms indicate promising performance of the method in the task of extracting endmembers from real hyperspectral data. In our experiments, we use laboratory-simulated forest scenes with known endmembers and fractional abundances due to their acquisition in a controlled environment using a real hyperspectral imaging instrument.

Index Terms— Spectral unmixing, endmember extraction, abundance estimation, minimum volume enclosing simplex, laboratory-simulated forest scenes.

1. INTRODUCTION

Spectral unmixing is an important tool for remotely sensed hyperspectral data exploitation [1]. Due to the spatial resolution of the sensor, most of the pixel (vectors) collected by imaging spectrometers such as NASA Jet Propulsion Laboratory's Airborne Visible Infra-Red Imaging Spectrometer (AVIRIS) [2] –with spatial resolution of 20 meters per pixel and 224 spectral bands comprised between 0.4 and 2.5 microns– are highly mixed in nature. Let us assume that a hyperspectral scene contains $i = 1, \ldots, m$ spectral bands and

$k = 1, \ldots, r$ pixel vectors. Each of the pixel vectors in the scene can be modeled using the following expression:

$$y = Xa + \epsilon, \tag{1}$$

where y is a pixel vector with dimensions $m \times 1$, X is a matrix with dimensions $m \times n$ containing a set of n pure spectral constituents (*endmembers*), and a is a $1 \times n$ vector containing the fractional abundance of each of the n endmembers in the pixel y. Finally, ϵ is a $m \times 1$ vector of white noise with standard deviation σ. The final goal of the model is to recover the matrix X and the fractional abundance a_k of each observed pixel k. To do so, usually two aspects need to be minimized: noise (in least squares fashion) and the volume of the simplex spanned by the columns of matrix X. Moreover, the abundance should be positive for each pixel given data y_k in the $m \times r$ matrix of band observations. The question is how to deal with least squares and minimum volume in such a way that the estimation is unbiased, i.e. the expected value of the estimator is the real value. When applying the idea of least squares during the estimation procedure we find the first problem in the sense that, very often, the number of endmembers is not known in advance. Therefore, techniques such as principal component analysis (PCA) [3] or the minimum noise fraction (MNF) [4] can be used for this purpose. In other words, if we assume that n endmembers are sufficient to characterize mixed pixels in the scene, the goal is to discover an $n - 1$ dimensional subspace responsible for the main variations, while the rest of the m dimensional space can be considered noise.

Over the last years, several algorithms have been developed for automatic or semiautomatic estimation of endmembers in matrix X by assuming that the input hyperspectral data set contains at least one pure pixel for each distinct material present in the scene, and therefore a search procedure aimed at finding the most spectrally pure signatures in the input scene is feasible. Techniques include the pixel purity index (PPI) [5], N-FINDR [6], iterative error analysis (IEA) [7], and an orthogonal subspace projection (OSP) technique in [8]. However, given the spatial resolution of state-of-the-art imaging spectrometers such as AVIRIS, the presence of pure pixels in collected hyperspectral data may not be feasi-

ble. As a result, other methods have been developed for endmember extraction that do not assume the presence of pure pixels in the input data, including minimum volume transform (MVT) [9], convex cone analysis (CCA) [10], optical real-time adaptive spectral identification system (ORASIS) [11], and a minimum volume constrained nonnegative factorization method (MVCNF) [12]. None of these methods incorporates the fractional abundance estimation as an internal step of the endmember extraction technique, and need an external abundance estimation method such as the fully constrained linear spectral unmixing (FCLSU) [13], which imposes abundance non-negativity and sum-to-one constraints, or the unconstrained linear spectral unmixing (ULSU) [14], which does not impose such constraints when estimating endmember fractional abundances.

In this paper, we present a new method called MINVEST for endmember estimation which adopts a hierarchical vision of the spectral unmixing problem: first, we use PCA to reduce data dimensionality and, second, we minimize the volume of an enclosing simplex in the reduced space while estimating the fractional abundance of vertices in simultaneous fashion. This approach is compared with the N-FINDR algorithm (which finds the simplex of maximum volume that can be inflated within the data) in different hyperspectral image analysis scenarios, considering that pure pixels are present (and not present) in the original data.

2. MINIMUM ENCLOSING SIMPLEX VERSUS MAXIMUM VOLUME SIMPLEX

Our unmixing method can be summarized as follows. First of all the data are centralized by the mean $\overline{y}$, such that the columns of Y consist of centralized observations $y_k - \overline{y}$. The observed variation in the spectral data $Y^T Y$ is approximated by $(CZ)^T CZ$ where C is an $m \times (n-1)$ matrix of principal components and Z is $(n-1) \times r$ a so-called score matrix. In direction c_1 we have the biggest variation, in direction c_2 the second biggest etc. Essentially we have reduced model (1) to

$$z = Va + \xi, \qquad (2)$$

where we expect the endmembers X to lay in the space $<C> + \overline{y}$ spanned by the columns of C. We should keep in mind that C represents an estimate of the space in which the endmember spectra X are located, $X = CV + \overline{y}$. To put it in another way, with absence of noise the estimate of C represents the space spanned by $X - \overline{y}\mathbf{1}^T$, where $\mathbf{1}$ is the all-ones vector of appropriate dimension. With noise, ξ is now the projection of ϵ on $<C>$ and therefore its components are independently Gaussian distributed. To be consistent, we should theoretically notice that $y = Cz + \overline{y} + \zeta$ where ζ is the part of ϵ projected on the orthoplement of $<C>$; $\epsilon = \xi + \zeta$. From these detailed statistical observations we will use the idea that the noise of z is component-wise independent.

In [12], an elegant matrix factorization approach that simultaneously minimizes least squares and the simplex volume is proposed. However, according to our experience these objectives might be conflicting. For volume reduction it is good to add a direction without variation to the principal components; zero variation gives zero volume. In turn, the least squares idea gives that we look for directions with maximum variation. In order to address this issue, we follow an approach often found in previous literature. First, we minimize noise and estimate the plane in which the n endmembers are lying. Secondly, in that plane, we minimize the volume of the resulting simplex such that it encloses the projections of the observed bands of the pixels. The N-FINDR algorithm [6] follows a similar approach where the volume of the simplex is maximized (instead of minimized) on the projected plane. In this regard, our approach can be seen as opposite to the one proposed in N-FINDR, which maximizes the volume of the simplex spanned by the endmembers in the projected plane. Instead, we aim at finding the enclosing simplex with minimum volume, facing the problem as a global optimization procedure [15]. This procedure, along with the possibility to obtain the fractional abundances of endmembers in simultaneous fashion, will be explained in more detail in the full paper.

3. EXPERIMENTAL RESULTS

In this section we use a set of laboratory simulated data sets in order to test the accuracy of the presented approach in both endmember extraction and fractional abundance estimations in a laboratory controlled analysis scenario. The data sets were acquired (in the laboratory) from artificial forest scenes [16], using the Compact Airborne Spectrographic Imaging (CASI) system. Two kinds of objects, opaque and translucent, were mounted on stems to simulate forest crowns on trunks. These simulated "trees" were randomly placed on a mounting board covered with a green background. The dimensions of tree crowns for opaque and translucent trees ranged from 1.3 cm to 1.7 cm. Canopies of both opaque and translucent trees were designed with sparse and dense populations. For the sparse population, 40 trees were planted in an area of 40 cm by 40 cm, while 100 trees were planted in the same area for the dense population. The scene illumination in this simulation was generated using a 100 W tungsten lamp and illumination angle of 40 degrees. Four hyperspectral images (labeled as CASI01_01 to CASI01_04) corresponding to all possible combinations of type of tree (opaque versus translucent) and type of distribution (dense versus sparse) were acquired by CASI, a pushbroom imager, by moving the entire scene perpendicularly at a constant rate with respect to the CASI field-of view. The scenes (see Fig. 1) were acquired in 72 spectral channels covering the spectral region from 414 to 914 nm, at nominal spectral resolution of 7.5 nm. The spatial resolution in the direction of across track is 0.27 cm. The Spreading of

Photons for Radiation INTerception (SPRINT) canopy model was used to estimate the fractional abundances of the three main constituents (sunlit tree, shadow and background) in the scenes [17]. In our experiments, the SPRINT-derived fractional abundances will be used to assess the quality of fractional abundances estimated by our method [18].

Table 1 shows the fractional abundances estimated by unconstrained (LSU) and fully constrained (FCLSU) linear spectral unmixing algorithms using the endmembers provided by MINVEST and N-FINDR. In all experiments, the quality of fractional abundances was assessed using the abundance estimations provided by the SPRINT canopy model (also reported in the Table 1). The most similar fractional abundance estimations across all tested methods with regards to SPRINT are shown in bold typeface. In order to interpret the results in Table 1, let us first focus on the scene with opaque trees and sparse population (CASI01_01). The errors in the fractions of the endmembers obtained by MINVEST (using both LSU and FCLSU) with regards to SPRINT are smaller than those obtained by N-FINDR for the background and shadow constituents, while the errors for the sunlit tree constituent are similar to SPRINT in all considered methods. Similarly, for the scene with translucent trees and sparse population (CASI01_02), the errors in the fractions of the endmembers obtained by MINVEST (using both LSU and FCLSU) are always smaller than the errors in the fractions of the endmembers obtained by N-FINDR.

If we now focus on the scenes with dense population (CASI01_03 and CASI01_04), Table 1 reveals that in those cases the fractions of the endmembers estimated by N-FINDR are generally the most similar to those estimated by SPRINT, regardless of whether LSU or FCLSU is used to estimate the final abundance fractions. This is probably due to the fact that a denser tree population increases the probability of finding pure pixels associated to sunlit trees in the scene, and this increases the accuracy of fractional estimations from N-FINDR endmembers for this particular constituent since N-FINDR assumes the presence of pure instances of each component in the scene. A similar effect is observed for the background endmember, which is better characterized from the endmembers obtained by N-FINDR in the scene with opaque trees and also in the scene with translucent trees. However, the most accurate estimate for the shadow endmember in the scenes with dense population is obtained from the MINVEST endmember. Since the shadow is generally mixed with trees (especially in the scenes with translucent trees) and background (in all cases), this observation allows us to conclude that MINVEST may be more effective than N-FINDR in the characterization of endmembers that do not appear in pure form in the scene. On the other hand, the N-FINDR seems to provide more accurate endmembers when pure pixels of the associated constituent are present in the scene.

Since most of the pixels in hyperspectral scenes are mixed due to insufficient spatial resolution to separate all spectrally distinct constituents and other phenomena, the aforementioned observations point out the potential of MINVEST in order to characterize highly mixed pixels in hyperspectral scenes and suggest that a combined use of both algorithms (MINVEST and N-FINDR) might also be possible in order to obtain an improved characterization of the full scene. Although the results obtained in this experiment are encouraging, further results with real data sets collected in a real (not laboratory simulated) environment are necessary in order to fully substantiate the utility of MINVEST in hyperspectral imaging applications. These results with real hyperspectral scenes will be included in the final version of the paper.

4. ACKNOWLEDGEMENT

5. REFERENCES

[1] J. B. Adams, M. O. Smith, and P. E. Johnson, "Spectral mixture modeling: a new analysis of rock and soil types at the Viking Lander 1 site," *Journal of Geophysical Research*, vol. 91, pp. 8098–8112, 1986.

[2] R. O. Green, M. L. Eastwood, C. M. Sarture, T. G. Chrien, M. Aronsson, B. J. Chippendale, J. A. Faust, B. E. Pavri, C. J. Chovit, M. Solis, et al., "Imaging spectroscopy and the airborne visible/infrared imaging spectrometer (AVIRIS)," *Remote Sensing of Environment*, vol. 65, no. 3, pp. 227–248, 1998.

[3] J. A. Richards and X. Jia, *Remote Sensing Digital Image Analysis: An Introduction*, Springer, 2006.

[4] D. Lee and H. S. Seung, "Learning the parts of objects by non-negative matrix factorization," *Nature*, vol. 401, pp. 788–791, 1999.

[5] J. W. Boardman, F. A. Kruse, and R. O. Green, "Mapping Target Signatures Via Partial Unmixing of Aviris Data," *Proc. JPL Airborne Earth Sci. Workshop*, pp. 23–26, 1995.

[6] M. E. Winter, "N-FINDR: an algorithm for fast autonomous spectral end-member determination in hyperspectral data," *Proc. SPIE Image Spectrometry V*, vol. 3753, pp. 266–277, 2003.

[7] R. A. Neville, K. Staenz, T. Szeredi, J. Lefebvre, and P. Hauff, "Automatic endmember extraction from hyperspectral data for mineral exploration," *Proc. 21st Canadian Symp. Remote Sens.*, pp. 21–24, 1999.

CASI01_01 **CASI01_02** **CASI01_03** **CASI01_04**
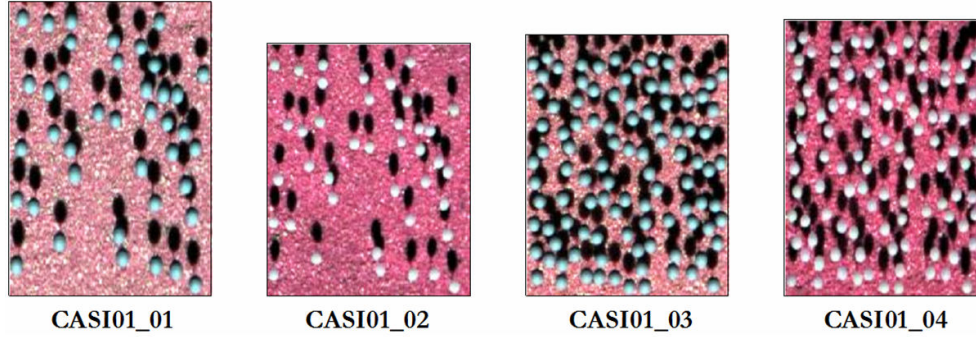
Fig. 1. False color images of the CASI laboratory scenes formed using band 50 (770 nm) as red, band 30 (618 nm) as green, band 20 (543 nm) as blue.

Table 1. Fractional abundance estimations provided by different methods for the main constituents in the CASI scenes. The most similar estimations with regards to the SPRINT canopy model are shown in bold typeface.

Hyperspectral Scene	Endmember signature	N-FINDR (LSU)	N-FINDR (FCLSU)	MINVEST (LSU)	MINVEST (FCLSU)	SPRINT model
CASI01_01	Sunlit tree	0.106	**0.108**	0.090	0.089	0.109
Sparse,	Background	0.683	0.680	**0.726**	**0.726**	0.723
opaque trees	Shadow	0.210	0.211	**0.183**	**0.183**	0.167
CASI01_02	Sunlit tree	0.062	0.062	**0.068**	**0.068**	0.104
Sparse,	Background	0.790	0.787	0.771	**0.768**	0.701
translucent trees	Shadow	0.146	0.150	0.160	**0.162**	0.194
CASI01_03	Sunlit tree	**0.183**	0.181	0.159	0.157	0.294
Dense,	Background	**0.354**	0.352	0.338	0.336	0.383
opaque trees	Shadow	**0.462**	0.465	0.502	0.506	0.318
CASI01_04	Sunlit tree	**0.169**	**0.169**	0.150	0.151	0.279
Dense,	Background	0.309	**0.313**	0.499	0.487	0.357
translucent trees	Shadow	0.521	0.517	0.349	**0.361**	0.362

[8] H. Ren and C.-I Chang, "Automatic spectral target recognition in hyperspectral imagery," *IEEE Transactions on Aerospace and Electronic Systems*, vol. 39, no. 4, pp. 1232–1249, 2003.

[9] M. D. Craig, "Minimum-volume transforms for remotely sensed data," *IEEE Transactions on Geoscience and Remote Sensing*, vol. 32, pp. 542–552, 1994.

[10] A. Ifarraguerri and C.-I. Chang, "Multispectral and hyperspectral image analysis with convex cones," *IEEE Transactions on Geoscience and Remote Sensing*, vol. 37, pp. 756–770, 1999.

[11] J. H. Bowles, P. J. Palmadesso, J. A. Antoniades, M. M. Baumback, and L. J. Rickard, "Use of filter vectors in hyperspectral data analysis," *Proc. SPIE Infrared Spaceborne Remote Sensing III*, vol. 2553, pp. 148–157, 1995.

[12] L. Miao and H. Qi, "Endmember extraction from highly mixed data using minimum volume constrained nonnegative matrix factorization," *IEEE Transactions on Geoscience and Remote Sensing,*, vol. 45, pp. 765–777, 2007.

[13] D. Heinz and C.-I Chang, "Fully constrained least squares linear mixture analysis for material quantifica-

tion in hyperspectral imagery," *IEEE Transactions on Geoscience and Remote Sensing*, vol. 39, pp. 529–545, 2001.

[14] C.-I Chang, *Hyperspectral Imaging: Techniques for Spectral Detection and Classification*, Kluwer Academic/Plenum Publishers: New York, 2003.

[15] E. M. T. Hendrix and B. G. Toth, *Introduction to Nonlinear and Global Optimization*, Springer, Cambridge, 2010.

[16] B. Hu, J. R. Miller, J. Wang, and N. S. Goel, "Investigation of linear spectral mixtures of the reflectance spectra using laboratory simulated forest scenes," *Proc. IEEE International Geoscience and Remote Sensing Symposium*, vol. 3, pp. 1535–1537, 2002.

[17] N. S. Goel and R. L. Thompson, "A snapshot of canopy reflectance models and a universal model for the radiation regime," *Remote Sensing Reviews*, vol. 18, pp. 197–225, 2000.

[18] J. Plaza and A. Plaza, "Spectral mixture analysis of hyperspectral scenes using intelligently selected training samples," *IEEE Geoscience and Remote Sensing Letters*, vol. 7, pp. 1–5, 2010.